REPORT DOCUMENTATION PAGE

Form Approved OMB NO. 0704-0188

1. REPORT DATE (DD-MM-YYYY)	2. REPORT TYPE	3. DATES COVERED (From - To)
23-06-2008	Final Report	15-May-2006 - 14-Feb-2007

4. TITLE AND SUBTITLE
Equation of state of ballistic gelatin

5a. CONTRACT NUMBER
W911NF-06-1-0170

5b. GRANT NUMBER

5c. PROGRAM ELEMENT NUMBER

6. AUTHORS
Muhetaer Aihaiti, Russell J. Hemley

5d. PROJECT NUMBER

5e. TASK NUMBER

5f. WORK UNIT NUMBER

7. PERFORMING ORGANIZATION NAMES AND ADDRESSES
Carnegie Institution of Washington
5251 Broad Branch Rd.

Washington, DC 20015 -

8. PERFORMING ORGANIZATION REPORT NUMBER

9. SPONSORING/MONITORING AGENCY NAME(S) AND ADDRESS(ES)
U.S. Army Research Office
P.O. Box 12211
Research Triangle Park, NC 27709-2211

10. SPONSOR/MONITOR'S ACRONYM(S)
ARO

11. SPONSOR/MONITOR'S REPORT NUMBER(S)
50533-EG.1

12. DISTRIBUTION AVAILIBILITY STATEMENT
Approved for Public Release; Distribution Unlimited

13. SUPPLEMENTARY NOTES
The views, opinions and/or findings contained in this report are those of the author(s) and should not contrued as an official Department of the Army position, policy or decision, unless so designated by other documentation.

14. ABSTRACT
We determined the equation of state for ballistic gelatin using the Brillouin scattering spectroscopy with a diamond anvil cell by measuring the pressure dependence of the sound velocities from ambient pressure to 12 GPa at room temperature. We extended these measurements to a temperature range of 0 to 100 °C between ambient and 12 GPa. We analyzed the Brillouin data using a high temperature Vinet equation of state and obtained the bulk modulus, its pressure derivative, thermal expansion coefficient and the temperature derivative of bulk modulus at ambient pressure. We also applied the Mie-Gruneisen method to the P, V, T data and obtained Gruneisen parameter, Debye temperature and its thermal pressures

15. SUBJECT TERMS
equation of state, high pressure, Brillouin spectroscopy, gelatin

16. SECURITY CLASSIFICATION OF:			17. LIMITATION OF ABSTRACT	15. NUMBER OF PAGES	19a. NAME OF RESPONSIBLE PERSON
a. REPORT	b. ABSTRACT	c. THIS PAGE			Russell Hemley
U	U	U	SAR		19b. TELEPHONE NUMBER 202-478-8957

Report Title

Equation of state of ballistic gelatin

ABSTRACT

We determined the equation of state for ballistic gelatin using the Brillouin scattering spectroscopy with a diamond anvil cell by measuring the pressure dependence of the sound velocities from ambient pressure to 12 GPa at room temperature. We extended these measurements to a temperature range of 0 to 100 °C between ambient and 12 GPa. We analyzed the Brillouin data using a high temperature Vinet equation of state and obtained the bulk modulus, its pressure derivative, thermal expansion coefficient and the temperature derivative of bulk modulus at ambient pressure. We also applied the Mie-Gruneisen method to the P, V, T data and obtained Gruneisen parameter, Debye temperature and its thermal pressures for the gelatin.

List of papers submitted or published that acknowledge ARO support during this reporting period. List the papers, including journal references, in the following categories:

(a) Papers published in peer-reviewed journals (N/A for none)

Number of Papers published in peer-reviewed journals: 0.00

(b) Papers published in non-peer-reviewed journals or in conference proceedings (N/A for none)

Number of Papers published in non peer-reviewed journals: 0.00

(c) Presentations

2007 Stewardship Science Academic Alliances (SSAA) Symposium;
February 05 to 08 2007 (Washington DC)
Sponsored by the national nuclear security administration

"High pressure Brillouin scattering studies of polymers"
by "M. Aihaiti, L. L. Stevens, E. B. Orler, D. M. Dattelbaum, H. -K. Mao, and R. J. Hemley"

Number of Presentations: 1.00

Non Peer-Reviewed Conference Proceeding publications (other than abstracts):

Number of Non Peer-Reviewed Conference Proceeding publications (other than abstracts): 0

Peer-Reviewed Conference Proceeding publications (other than abstracts):

Number of Peer-Reviewed Conference Proceeding publications (other than abstracts): 0

(d) Manuscripts

Manuscript submission is on hold

Number of Manuscripts: 0.00

Number of Inventions:

Graduate Students

NAME	PERCENT_SUPPORTED
FTE Equivalent:	
Total Number:	

Names of Post Doctorates

NAME	PERCENT_SUPPORTED
Muhetaer Aihaiti	0.50
FTE Equivalent:	**0.50**
Total Number:	**1**

Names of Faculty Supported

NAME	PERCENT_SUPPORTED	National Academy Member
Russell J. Hemley	0.50	Yes
FTE Equivalent:	**0.50**	
Total Number:	**1**	

Names of Under Graduate students supported

NAME	PERCENT_SUPPORTED
FTE Equivalent:	
Total Number:	

Student Metrics

This section only applies to graduating undergraduates supported by this agreement in this reporting period

The number of undergraduates funded by this agreement who graduated during this period:	0.00
The number of undergraduates funded by this agreement who graduated during this period with a degree in science, mathematics, engineering, or technology fields:.....	0.00
The number of undergraduates funded by your agreement who graduated during this period and will continue to pursue a graduate or Ph.D. degree in science, mathematics, engineering, or technology fields:.....	0.00
Number of graduating undergraduates who achieved a 3.5 GPA to 4.0 (4.0 max scale):	0.00
Number of graduating undergraduates funded by a DoD funded Center of Excellence grant for Education, Research and Engineering:	0.00
The number of undergraduates funded by your agreement who graduated during this period and intend to work for the Department of Defense	0.00
The number of undergraduates funded by your agreement who graduated during this period and will receive scholarships or fellowships for further studies in science, mathematics, engineering or technology fields:	0.00

Names of Personnel receiving masters degrees

NAME
Total Number:

Names of personnel receiving PHDs

NAME

Total Number:

Names of other research staff

NAME PERCENT_SUPPORTED

FTE Equivalent:

Total Number:

Sub Contractors (DD882)

Inventions (DD882)

Equation of state of ballistic gelatin

Muhetaer Aihaiti and Russell J. Hemley

Geophysical Laboratory, Carnegie Institution of Washington
5251 Broad Brach Rd., NW Washington DC 20015

Table of Contents

Summary:

We determined the equation of state for ballistic gelatin using the Brillouin scattering spectroscopy with a diamond anvil cell by measuring the pressure dependence of the sound velocities from ambient pressure to 12 GPa at room temperature. We extended these measurements to a temperature range of 0 to 100 °C between ambient and 12 GPa. We analyzed the Brillouin data using a high temperature Vinet equation of state and obtained the bulk modulus, its pressure derivative, thermal expansion coefficient and the temperature derivative of bulk modulus at ambient pressure. We also applied the Mie-Gruneisen method to the *P*, *V*, *T* data and obtained Gruneisen parameter, Debye temperature and its thermal pressures for the gelatin.

I. Introduction

The ubiquity of polymer-like materials in science and society is a clear testament to the importance of these unique materials. The diversity of polymeric-material applications, which range from optics and electronics to garden hoses and soda bottles, provides a practical impetus for fundamental research in polymer physics and chemistry. While the chemistry of polymeric chain formation is primarily dictated by the reactivity of the monomer units, the resultant physical properties of a given polymer are highly reliant on network topology and presence or absence of filler materials. In addition, external stimuli, such as variable temperatures and pressure, have pronounced influence on their mechanical behavior. Examples include thermal aging phenomena, pressure-induced crystallization, shock-compressed polymorphism, and thermoplasticity. Most of the biomaterials (such as gelatin) can be analogous to polymers.

The term “gelatin” is used to refer to a yellow-white powder, 100% protein, extracted by acid or base hydrolysis from collagen, the main matrix material of animal skin, bone, and connective tissue. The term also refers to a water solution of this powder. Gelatin is an aggregate, meaning there is no single molecular size and formula. Instead, gelatin is a collection of large protein molecules similar to amino acid composition. In a given gelatin sample, the molecular weight ranges between 17,000 and 300,000 Daltons. Thus only the average molecular weight can be used in characterization of the gelatin.

Gelatin, one of the most versatile hydrocolloids, has a wide variety of uses in many industries. It is used in the food industry for making edibles such as desserts, marshmallows, jellies, and aspics. It is used by the pharmaceutical industry to manufacture capsules, tablets, and bandages. Gelatin is also an important raw material in

the photographic industry. Another use for gelatin is as the “model” of human tissue in bullet penetration experiments (Ref. 1). This is the so-called “ballistic gelatin.” It is necessary to obtain the equation of state (EOS) for ballistic gelatin to describe its elastic behavior under pressure.

Since sound waves are intimately associated with changes in pressure and density, Brillouin scattering measurements can provide precise pressure-volume data for a variety of materials. The work presented here supplies a necessary extension to the currently limited EOS data available for gelatin. In-situ sound velocities are directly related to elastic constants which, in turn, arise directly from the curvature of an intermolecular potential. Given these relationships, sound velocity measurements can provide useful insight into the microscopic structure of a material. The EOS and mechanical properties of gelatin – have been determined from ambient pressure to approximately 12 GPa using a diamond-anvil cell (DAC) in conjunction with Brillouin scattering. Besides elastic properties and *P-V* EOS data, Brillouin scattering can also provide insight into the dynamic relaxation processes in gelatin (Ref. 2).

II. Experimental details

(1) **Diamond anvil cell**

Figure 1 shows the simple schematic diagram of DAC used in this experiment. It consists of three major components: the diamond anvils, a piston, and cylinder parts. The diamond anvils are separately fixed to the piston and cylinder parts. A metal gasket with a hole in its center is used as a sample chamber. When the piston and cylinder are pressed toward each other, the gasket as well as the pressure medium and samples will be compressed, which will generate pressure on the sample. In this experiment, we did not

use a pressure medium because gelatin itself is very soft and would play the role of pressure medium. We used a standard ruby fluorescence method to determine the pressure. The samples of gelatin (20%) are prepared with the methods described in Ref. 1. Gelatin samples are loaded into a DAC (Fig. 1) with no pressure medium added. Pre-indented (12 GPa) stainless gaskets with gasket hole of about 150 microns are used. Figure 1(b) shows some details of diamond anvils, gasket, and thermocouples.

(2) **Brillouin scattering system**

Brillouin light scattering is generally referred to as inelastic scattering of an incident optical wave field by thermally excited elastic waves in a sample. Light scattering from thermally excited acoustic waves was theoretically predicted by L. Brillouin (Ref. 3). Later, Gross (Ref. 4) experimentally confirmed the prediction in liquids and in crystals. Brillouin spectroscopy did not progress until the 1960s, due to a lack of intense light sources. In 1960, the invention of the laser solved the light source problem; since then, Brillouin light scattering techniques have earned reasonable attention and have been widely used in many research fields.

In the case of a transparent solid (crystals or glasses), the incident laser light will induce dynamic fluctuations in the strain field to bring about fluctuations in the dielectric constant, and these in turn translate into fluctuations in the refractive index due to the *elasto-optic scattering mechanism*. These fluctuating optical inhomogeneities result in inelastic scattering of the light as it passes through the solid. The phonons present inside a solid move in thermal equilibrium with very small amplitudes, creating fluctuations in the dielectric constant, which is viewed as a moving diffraction grating by an incident light wave. Therefore Brillouin scattering can be explained as a combination of Bragg

reflection and Doppler effect. The moving grating scatters the incident light giving rise to scattered photons with Doppler shifted frequencies $\Delta\nu$. Brillouin spectrum gives frequency shift ($\Delta\nu$) of the thermal phonon, and its wavelength (d space) can be determined from the experiment geometry. For instance, with n_i as the refractive index in the direction of incident light, n_s as the refractive index in the scattering direction, and υ as the velocity of acoustic phonons, the Brillouin shift $\Delta\nu$ is given as follows:

$$\Delta\nu = \frac{\upsilon}{\lambda}\sqrt{(n_i^2 + n_s^2 - 2n_i n_s \cos\theta)} \qquad (1)$$

where λ is the wavelength of incident light and θ is the scattering angle.

The simple schematic arrangement for a Micro-Brillouin scattering system is shown in Figure 2, and some experimental details can be found in Refs.5-10. This is a non-contact measurement technique that exploits light scattering to probe the elastic properties of liquids and solids (crystals). Light from a single mode Ar-ion laser (λ=514.5 nm) was used as the excitation source with the average power less than 100 mW. The sample was placed symmetrically with respect to the incoming and collected light such that the difference vector of the incoming and detected light was in the plane of the sample. The scattered light was collected by lens L2, analyzed by a 3+3 tandem Fabry-Perot interferometer, detected by a photon counting photomultiplier, and was outputted to a multichannel scalar (Fig. 2). Spectra were taken at each pressure and a temperature point, and collected for 10 to 120 minutes.

Figure 3 exhibits the symmetric scattering geometry employed in these experiments, the scattering angle was 80° degrees. Since samples were placed symmetrically with respect to the incoming and collected light, and for this particular

geometry the frequency shift of the incident light is independent of the refractive index of the samples, the Eq. (1) can be reduced to

$$\Delta\nu = (2\upsilon/\lambda)\sin(\theta/2), \qquad (2)$$

where υ is sound velocity, λ=514.5 nm (laser wavelength), and θ=80° is the scattering angle.

The temperature up to 100 °C was generated by a ribbon heater which wrapped around DAC as shown in Fig. 1(a). The temperature was measured by a thermocouple which was placed between the diamond anvil and the gasket (close to the sample) as shown in Fig.1(b). Since the heater was uniformly wrapped over the DAC body, the temperature could be considered as uniformly distributed. Since diamond is an excellent heat conductor, the measured temperature can be considered close enough to the sample temperature. The fluctuations of temperature were below ± 3 °C at 100 °C during the measurement.

III. Results

The microscopic photo images taken at pressure 0, 2.1, and 11 GPa, respectively are shown in Fig. 4. The images at 0 and 11 GPa show that the gelatin clearly is isotropic. However, the image at 2.1 GPa shows that the gelatin starts to crystallize at this pressure. The images at 2.1 and 11 GPa were taken during different runs of experiments. The resulting images can be understood as follows: the samples are compressed to around 2 GPa and stay at this pressure regime, the samples will crystallize; if they are compressed very quickly and pass through this pressure regime, the samples will not crystallize and will go to a glassy state.

A typical set of Brillouin spectra is shown in Figure 5. There are two pairs of peaks in each spectrum and an additional Rayleigh peak at zero frequency (elastic scattering). One pair of peaks corresponds to the longitudinal acoustic mode (L-mode), whereas the other pair corresponds to the transverse acoustic mode (T-mode).

In additions, figure 6 exhibits the pressure dependence of Brillouin frequency shifts at room temperature. Figure 7 shows the pressure dependence of sound velocities at selected temperatures between 273 and 373 K. Figure 8 shows the temperature dependence of sound velocities at selected pressures. Now, we have the pressures, temperatures, and sound velocity data (calculated from Eq. 2) between ambient and 12 GPa, 273 and 373 K. The *P-V-T* EOS fitting will be discussed in detail in the next section.

IV Discussion

(1) Density calculations

The gelatin can be considered as an isotropic material, we calculate the pressure dependence of density of gelatin using following equation (Ref. 2):

$$\rho - \rho_0 = \int_{P_0}^{P} \frac{\gamma}{\upsilon_L^2 - \frac{4}{3}\upsilon_T^2} dP, \qquad (3)$$

where ρ and ρ_0 are the density at pressure *P* and *P0* respectively, υ_L and υ_T are the longitudinal and transverse sound velocities respectively, and $\gamma = C_P / C_V \approx 1$ [Refs. 9, 10, 11] is the ratio of specific heat at constant pressure and constant volume.

To calculate the density changes from 0 to 100 °C between 0 and 12 GPa, we have to solve the following two problems first: (1) the initial density for each temperature

between 0 and 100 °C at ambient pressure; (2) the initial velocities for each temperature between 0 and 100 °C at ambient pressure.

We solved these problems as follow: (1) the initial density was measured at 30 °C at ambient pressure, ρ=0.991 +/- 0.006 g/cm^3. Our initial density is very close to the data from Ref. 12. We applied the T-dependence of density from Ref. 12 and extrapolated it up to 100 °C at ambient pressure. The result is shown in Fig. 9 with the inset table. (2) The initial sound velocity is 1340 m/s at 30 °C at ambient pressure. Since gelatin is not stable above 40 °C (Ref.1), it is difficult to measure the sound velocity above 40 °C at ambient pressure. Instead we measured the temperature dependence of sound velocity from 0 to 100 °C at 0.53 GPa as shown in figure 10. We assumed that the T-dependence of sound velocity at ambient pressure should be similar to the one obtained at 0.53 GPa due to the small pressure difference. Therefore, by using the T-dependence of sound velocity at 0.53 GPa and combined with the initial sound velocity measured at 30 °C at ambient pressure, we extrapolated the T-dependence of sound velocity from 0 to 100 °C at ambient pressure. The results are shown in Fig. 10 (b). Consequently, we calculated the pressure dependence of density (1/V) at each selected temperature. The results are shown in Figure 11 and table I. There are very small difference in density between -2 and 100 °C. In the next two sections, we will discuss how we analyze the *P-V-T* Brillouin data using high temperature Vinet EOS and the Mie-Gruneisen method.

(2) *P-V-T* EOS

The *P-V-T* EOS are needed in order to discuss the intermolecular interaction and potential for simple fluid or solid materials. However, in the case of gelatin, the EOS can only give us the average information about intermolecular interaction and potential. Here

we analyze the *P-V-T* data with two methods: one extends the room-T Vinet EOS to a higher temperature by considering the thermal expansion, the other is based on the idea of thermal pressure, which is that the total pressure on the sample is the sum of static pressure and pressure due to thermal expansions.

(a) **High temperature Vinet EOS**

Vinet equation of state is expressed as follow:

$$P = 3K_0[\frac{1-(V/V_0)^{1/3}}{(V/V_0)^{2/3}}]\exp[\frac{3}{2}(K_0^{'}-1)(1-(V/V_0)^{1/3})] \quad (4)$$

where K_0 is the bulk modulus, K_0' is its derivative at zero pressure, and V_0 is the initial volume at room temperature. We fitted the pressure dependence of density at room temperature by using the Vinet EOS with three parameters and obtained the bulk modulus of 4.9 GPa, its derivative at zero pressure of 8.2, and the initial volume of 1.004 (cm^3/g). For the temperature effect, the high temperature Vinet EOS incorporates temperature effect into the third order Vinet EOS, and is expressed as the following:

$$P = 3K_{0T}[\frac{1-(V/V_{0T})^{1/3}}{(V/V_{0T})^{2/3}}]\exp[\frac{3}{2}(K_{0T}^{'}-1)(1-(V/V_{0T})^{1/3})] \quad (5)$$

where K_{0T}, K_{0T}', and V_{0T} are isothermal bulk modulus, its pressure derivatives, and initial volume at temperature T and ambient pressure, respectively. Assuming that the second and third order pressure derivatives of the bulk modulus are negligible, then K_{0T} and K_{0T}' are given by the properties at ambient conditions

$$K_{0T} = K_0 + (\frac{\partial K_T}{\partial T})_P(T-302) \quad (6)$$

$$K_{0T}^{'} = K_0^{'} \quad (7)$$

where K_0 and K_0' are the isothermal values at ambient conditions. The temperature derivatives of the bulk modulus are assumed to be constant throughout the whole temperature range. Zero-pressure volume V_{0T} is expressed as

$$V_{0T} = V_0 \exp \int_{302}^{T} \alpha_T dT \quad (8)$$

$$\alpha_T = \alpha_0 + \alpha_1 T + \alpha_2 T^{-2} \quad (9)$$

where V_0 is the initial volume at ambient conditions, and α_T is the thermal expansion coefficient at ambient pressure, and expressed by constant parameters α_0, α_1, and α_2. Since the experiment was carried out in a relatively narrow temperature range from 0 to 100 °C, the coefficients α_1 and α_2 can be set to zero. The combination of Eqs. (5) to (9) is fitted to the *P-V-T* data. A least-squares fit, using program EOS-fit Version5.2 (Ref. 13), yielded: K_0=4.6 +/- 0.2 GPa, K_0'=8.7 +/- 0.2, V_0=1.004 +/- 0.002 cm^3/g, α_0=(40.4 +4.0) $\times 10^{-5}$ K^{-1}, and $(\frac{\partial K_T}{\partial T})_P$ = -0.009 +/- 0.002 $GPaK^{-1}$. We separately fitted the Vinet EOS to pressure dependence of density at each temperature. We obtained (V_{0T}, K_{0T}, K_{0T}') for each temperature; the results were summarized in Table II & III.

(b) Mie-Gruneisen model

According to the Mie-Gruneisen theory, the total pressure $P_{tot}(V, T)$ at a given volume and temperature can be expressed as a sum of static compression at a reference temperature $P_{st}(V, T_0)$ and the thermal pressure $\Delta P_{th}(V, T)$ at a given volume V:

$$P_{tot}(V,T) = P_{st}(V,T_0) + \Delta P_{th}(V,T) \quad (10)$$

For the static pressure term, P_{st}, we use the Vinet fit.

The Debye model can be used to describe thermal pressure term in (10). Indeed, it has been suggested that the Debye model is a good approximation for solids such as MgO

or $MgSiO_3$ or many other minerals. We only can assume that the Debye model may also be a possible approximation for gelatin due to its elastically isotropic properties. With this model, the first terms in (10) is:

$$P = 3K_0[\frac{1-(V/V_0)^{1/3}}{(V/V_0)^{2/3}}]\exp[\frac{3}{2}(K_0^{'}-1)(1-(V/V_0)^{1/3})] \quad (11)$$

and the second term is

$$\Delta P_{th}(V,T) = \frac{\gamma(V)}{V}[E_{th}(V,T) - E_{th}(V,T_0)] \quad (12)$$

where K_0 is the isothermal bulk modulus, K_0' is its pressure derivative, and γ is the Gruneisen parameter. The subscript zero denotes ambient conditions. The vibrational energy can be calculated from the Debye model

$$E_{th} = \frac{9nRT}{(\theta/T)^3}\int_0^{\theta/T}\frac{\xi^3}{e^{\xi}-1}d\xi \quad (13)$$

The Debye temperature is given by θ, n is the number of atoms in a formula unit, and R is the gas constant. The Gruneisen parameter γ is assumed to be a function of volume only

$$\gamma = \gamma_0(\frac{V}{V_0})^q \quad (14)$$

where q is assumed to be constant. The Debye temperature can also be described as a function of volume

$$\theta = \theta_0\exp(\frac{\gamma_0 - \gamma(V)}{q}) \quad (15)$$

In this approach, the fitting parameters are: V_0, K_0, K_0', γ_0, q, and θ_0. This EOS has the advantage that it yields higher order thermoelastic terms in an internally consistent way. The first three terms (V_0, K_0, K_0') are obtained from 300 K data. Although the EOS is not sensitive to the choice of θ_0, calculating the Debye temperature for gelatin is an important

step. In general, Debye temperature is calculated for crystalline structures (metal, crystals, and minerals [Ref. 11]) using the lattice vibrational properties. However, the gelatin does not have crystalline structure. We may be able to estimate the value for gelatin as follows: Since we measured the sound velocity at ambient pressure and room temperature and the longitudinal velocity υ_L=1340 m/s, shear velocity υ_T =0 m/s. υ_T can be replaced by υ_L and using the following equation

$$\frac{3}{\upsilon_D^3} = \frac{2}{\upsilon_T^3} + \frac{1}{\upsilon_L^3} \qquad (16)$$

we obtained the Debye velocity υ_D=1933 m/s. The Debye temperature can be expressed as follows:

$$\theta_0 = \frac{h}{K}\left(\frac{3N}{4\pi}\right)^{1/3}\left(\frac{\rho}{M/p}\right)^{1/3}\upsilon_D \qquad (17)$$

where k, h, and N are Boltzman's constant, Plank's constant, M is the molecular mass, p is the number of atoms in the molecular formula, and Avagadro's number, respectively. Since gelatin does not have crystalline structure, we use the initial volume at ambient conditions. The average weight of gelatin molecular is 175000 Dalton which equals to $3*10^{-22}$ kg. The number of molecules in initial volume is $3.33*10^{24}$. Using those numbers, we estimated the Debye temperature as: 100 K< θ_0 < 200 K.

The combination of Eqs (7)-(12) were fitted to the *P*-*V*-*T* data. Three different θ_0 (100, 150, and 200 K) were chosen. The fitting results remained unchanged. Consequently, θ_0 is set to 150 K. This allows us to obtain: K_0=4.9 +/- 0.2 GPa, K_0'=8.2 +/- 0.2, V_0=1.004 +/- 0.002 cm^3/g, Gruneisen parameter γ=0.17, and q=1 (fixed). The calculated pressures as well as the thermal pressures are shown in Table V. Figure 12 shows the thermal pressure as a function of temperature. For example, the thermal

pressure at 372 K and 9 GPa is about 0.6 GPa. This number is within the ±3σ of measured error in pressure (σ=0.2 GPa). This indicates that the temperature range in the current study is relatively narrow, in order to well constrain the Gruneisen parameter and its q, it is necessary to extend the temperature range up to or above 600 °C .

(c) **Elastic properties**

The isotropic material has two independent elastic constants: C_{11} and C_{12}. In general:

$$\rho \upsilon_L^2 = C_{11} \tag{18}$$

$$\rho \upsilon_T^2 = \frac{1}{2}(C_{11} - C_{12}) \tag{19}$$

where ρ is density, υ_L is the longitudinal sound velocity, and υ_T is the transverse sound velocity. The Poisson's ratio can be expressed as follows:

$$\sigma = \frac{\upsilon_L^2 - 2\upsilon_T^2}{2(\upsilon_L^2 - \upsilon_T^2)} \tag{20}$$

We calculated C_{11}, C_{12}, and σ as the function of pressure at room temperature shown in Fig. 13. They both increase linearly with pressure; C_{11} increases with pressure faster than C_{12}. On the other hand, the Poisson's ratio decreases with pressure. The value of Poisson's ratio is 0.36 at 10 GPa. It is comparable with that of silicate glass at the same pressure (Ref. 5).

Conclusion

We determined the EOS for ballistic gelatin using the Brillouin scattering spectroscopy using a diamond anvil cell to measure the pressure dependence of the sound velocities from ambient pressure to 12 GPa (in a 80° symmetric scattering geometry) at room temperature. We calculated the pressure dependence of elastic constants and

Poisson's ratio at room temperature. We extend this method to a temperature range of 0 to 100 °C between ambient pressure and 12 GPa. We analyzed the Brillouin data by using a high temperature Vinet EOS fitting to *P-V-T* data and obtained the thermal expansion coefficient (first-order approximation). We also used the Mie-Gruneisen method and obtained the Gruneisen parameter γ for gelatin.

Acknowledgments

This work was sponsored by ARL, AOL.

References:

1. http://www.vyse.com/gelatin_for_ballitic_testing.htm.

2. W. F. Oliver, C. A. Herbst, S. M. Lindsay, and G. H. Wolf, Phys. Rev. Lett. **67**, 2795 (1991).

3. Brillouin L., Diffusion de la lumiere et des rayonnes X par un corps transparent homogene; influence del'agitation thermique. *Ann. Phys.* (Paris) **17**, 88 (1922).

4. Gross, E., Change of wave-length of light due to elastic heat waves at scattering in liquids, *Nature* **126**, 400 (1930).

5. C. S. Zha, et al, Phys. Rev. B **50** 13105 (1994).

6. Ahart, M., A. Asthagiri, Z. G. Ye, P. Dera, H. K. Mao, R. E. Cohen and R. J. Hemley, Phys. Rev. B **75**, 144410 (2007).

7. Ahart, M., J. L. Yarger, K. M. Lantzky, S. Nakano, H. K. Mao and R. J. Hemley, *J. Chem. Phys.* **124**, 14502 (2006).

8. Sandercock, J. R., Trends in Brillouin-Scattering - Studies of Opaque Materials, Supported Films, and Central Modes, in *Light Scattering in Solids III. Recent Results* (eds. M. Cardona and G. Guntherodt) Berlin, Springer -Verlag., **51**, 173 (1982).

9. K. Matsuishi, et al, J. Phys.: Condens. Matter **14**, 10631 (2002).

10. Introduction to sloid state physics (sixth edition) by Charles Kittel, chapter 5, P101.

11. K. Matsuishi, E. Gregoryanz, H. –K. Mao, R. Hemley, J. Chem. Phys. **118**, 10683 (2003).

12. J. M. Brown, L. J. Slutsky, K. A. Nelson, L. T. Cheng, Science **241**, 65 (1988).

13. S. H. Shin, and T. S. Duffy, J. Geophys. Res. **105**, 25955 (2000).

14. Dana, (Los Alomos National Lab) personal communication.

15. R. J. Angle, Rev. in Mineral. Geochem. **41**, Mineral Soc. Of Am., Washington DC, P35, Ed., by R. Hazen, and R. Downs.

16. ARL report on gelatin (from Dr. Huang).

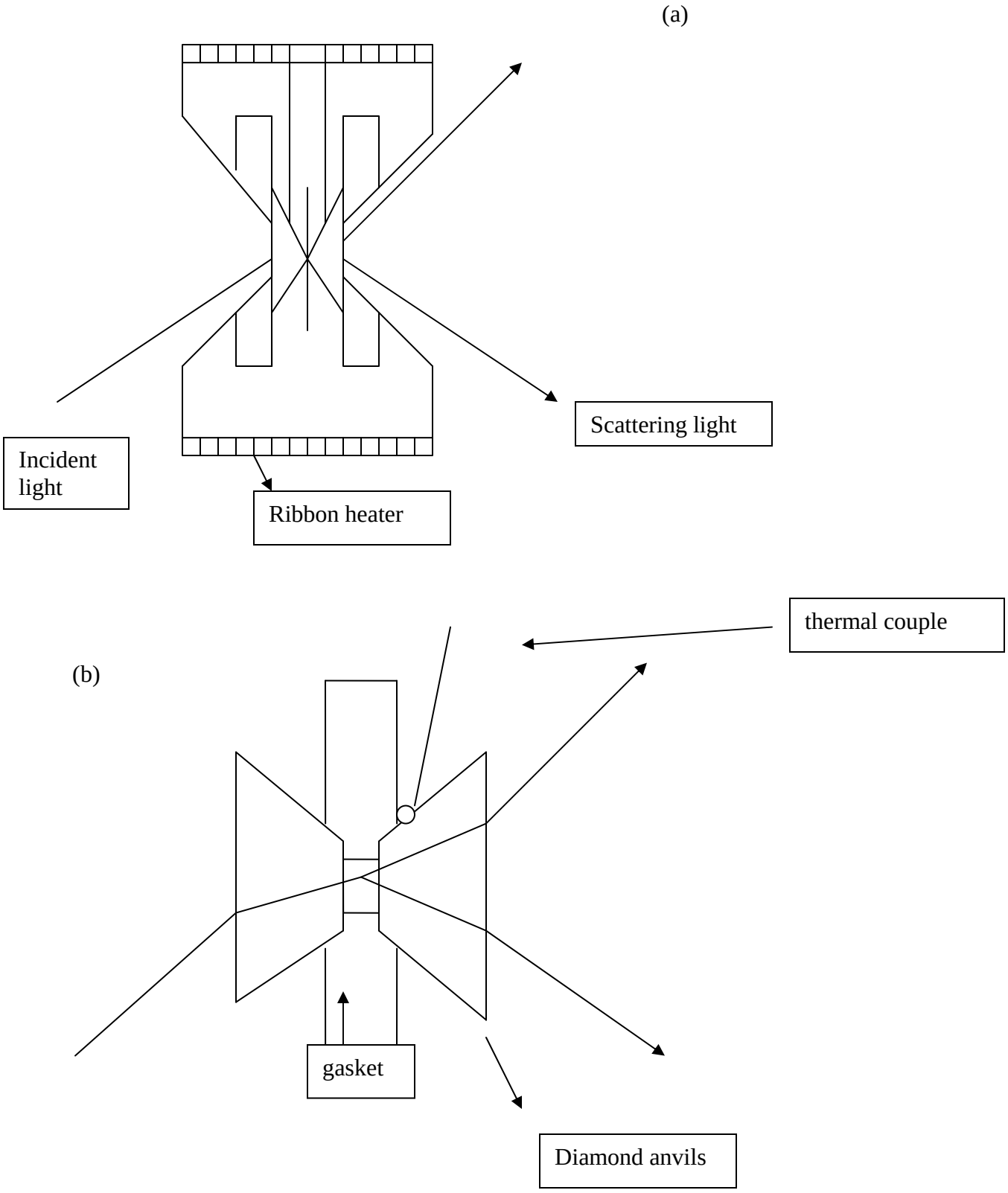

Figure 1. (a) Simple diagram of diamond anvile cell. The Brillouin scattering geometry is 80 degrees: symmetric scattering. (b) Diamond anvils.

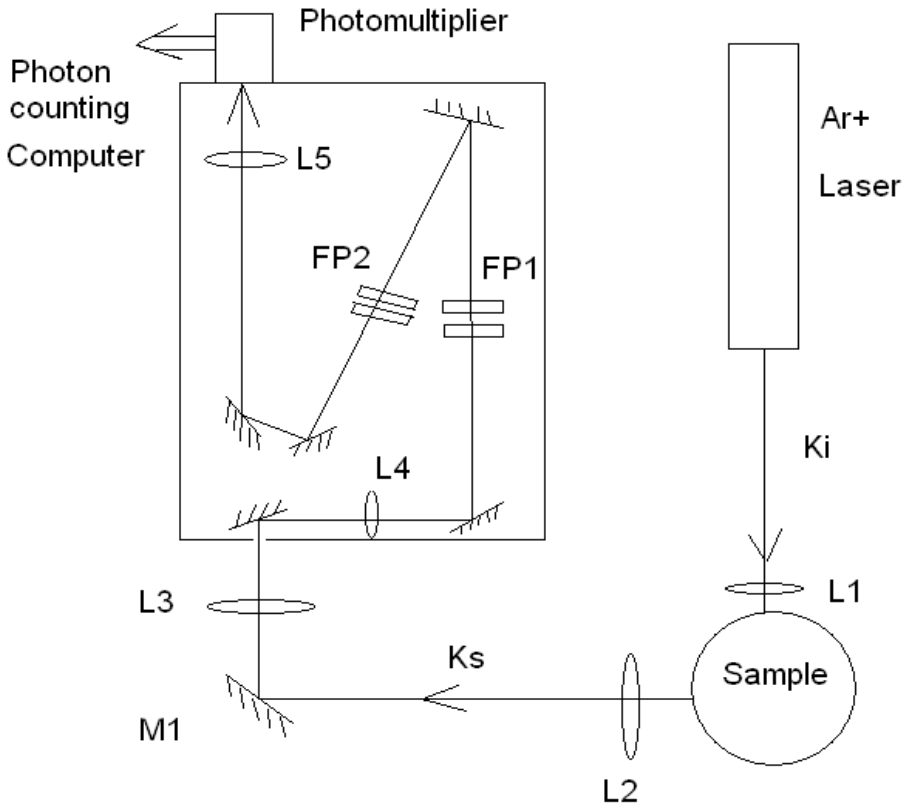

Figure 2. Simple diagram of Brillouin scattering system. Ar+ ion laser is operated at 514.5 nm and power is less than 100 mW.

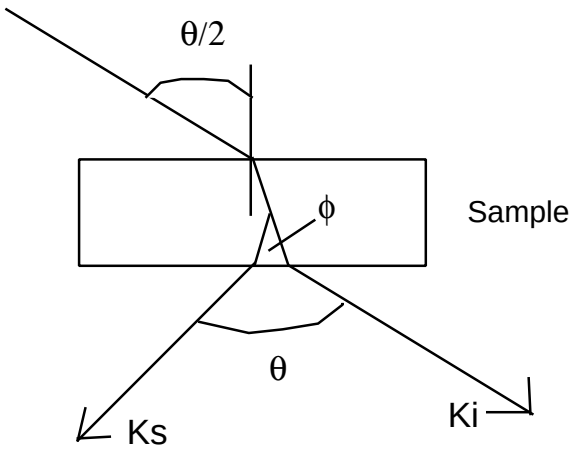

Figure 3. A diagram of the symmetric scattering geometry. The incident light enters the sample with the angle $\theta/2$, and by Snell's law the following equation will hold: $n_0\sin(\theta/2)=n\sin(\varphi/2)$, where n_0 is the refractive index of air and n is the refractive index of samples. Therefore the Brillouin shifts will have the following form: $\Delta\nu_{\varphi} = \frac{2n\upsilon}{\lambda}\sin(\varphi/2) = \frac{2\upsilon}{\lambda}\sin(\theta/2) = \Delta\nu_{\theta}$. The Brillouin shifts can be defined uniquely by the scattering angle between incident and scattering light.

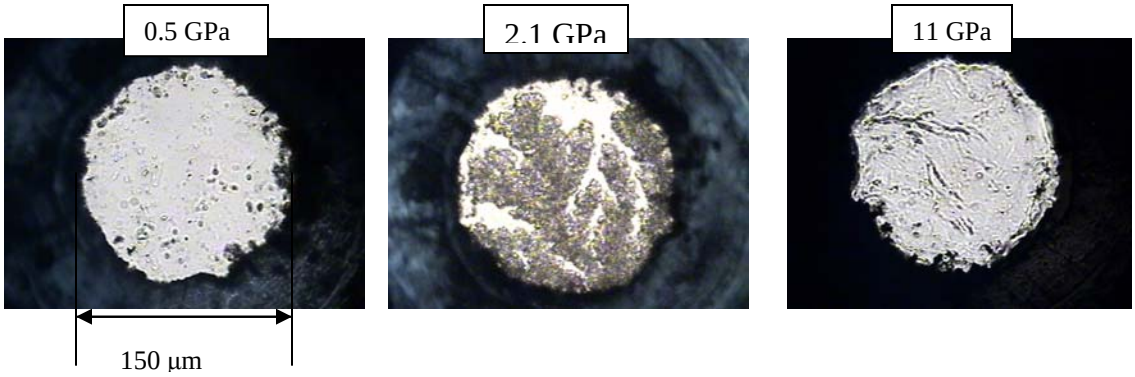

Figure 4. Photo image of gelatin in a DAC cell at selected pressure.

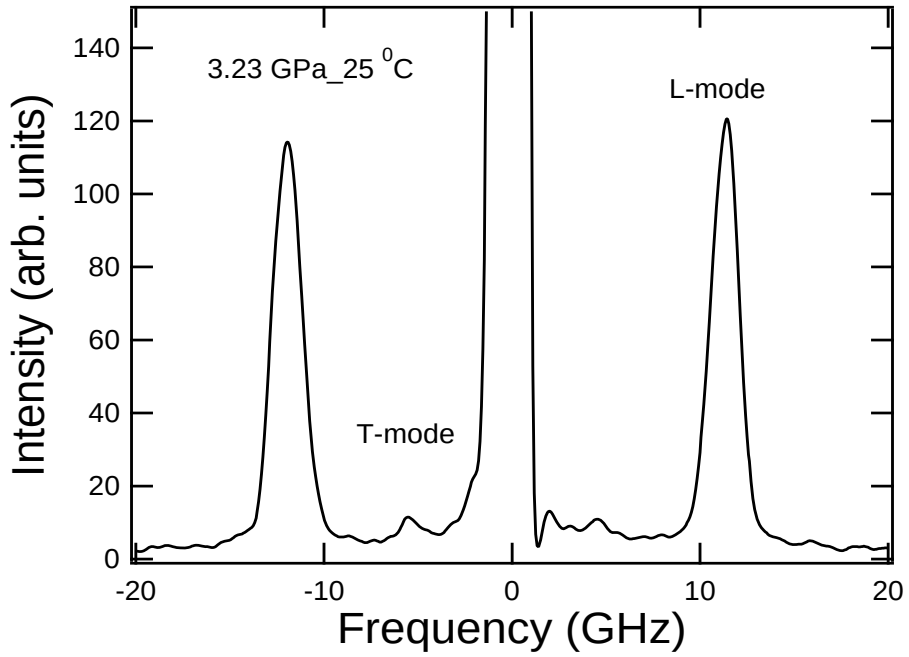

Figure 5. A typical Brillouin spectrum. The elastic scattering line at the zero frequency. The Brillouin lines at around 5 and 12.5 GHz for transverse and longitudinal acoustic mode, respectively.

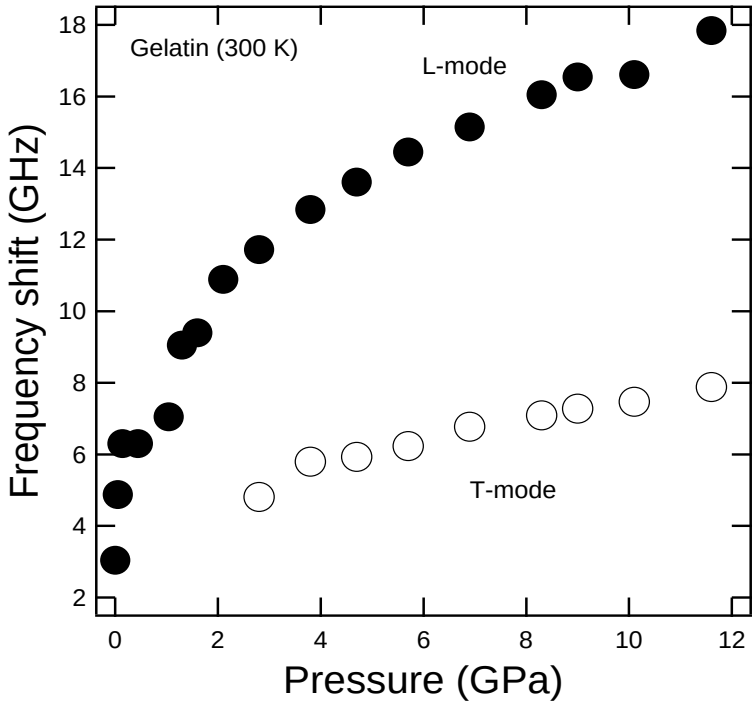

Figure 6. Pressure dependence of the Brillouin frequency shifts. Solid and open circles correspond to the longitudinal and transverse acoustic mode, respectively.

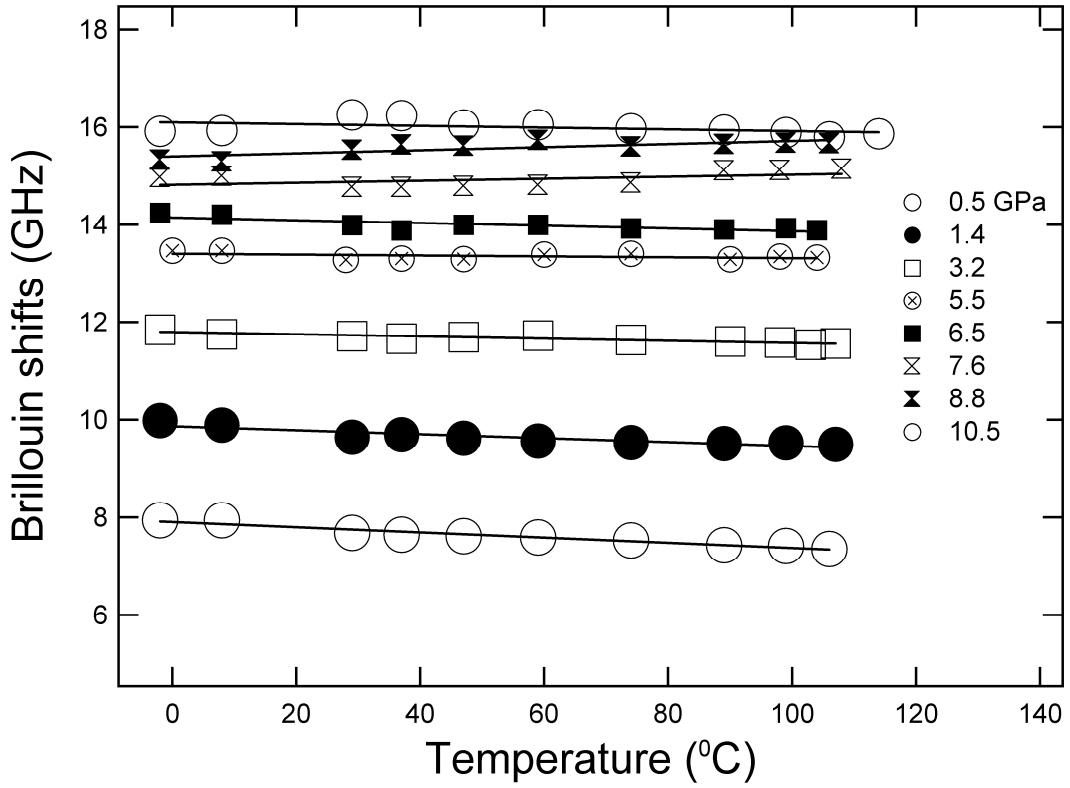

Figure 7. The temperature dependence of Brillouin shifts which correspond to the longitudinal mode at selected pressure. Symbols are experiment data and lines are the linear fits.

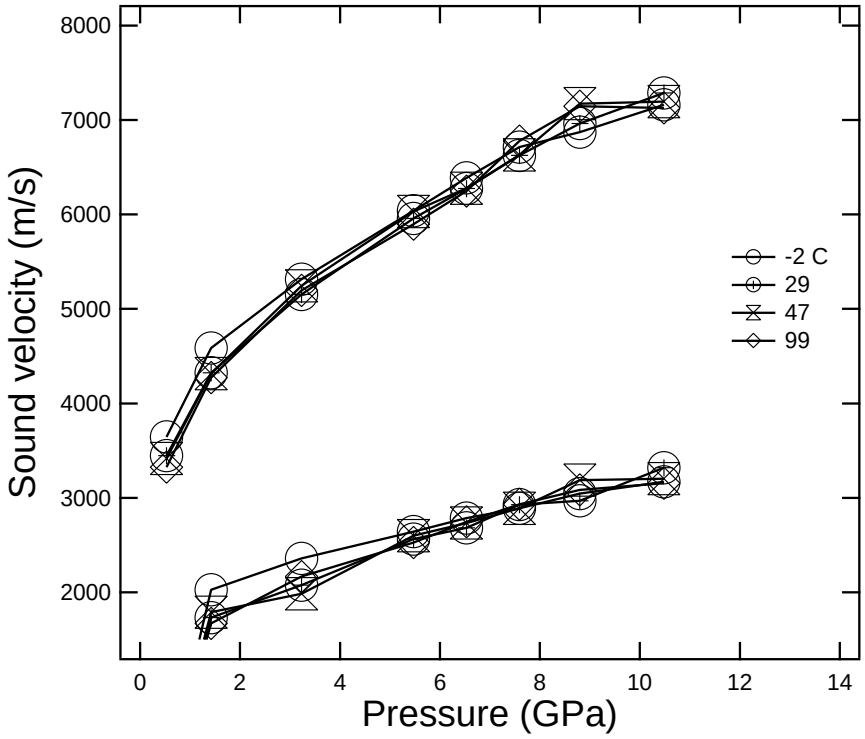

Figure 8. Pressure dependence of sound velocity at selected temperatures. Symbols are the experiment data and lines are the guide to eyes.

Point	'Temperature (C)'	'Density (g/cm3)'	
0	30	0.994728	
1	34	0.993345	
2	37	0.991375	
3	40	0.990688	
4	43	0.989413	
5			

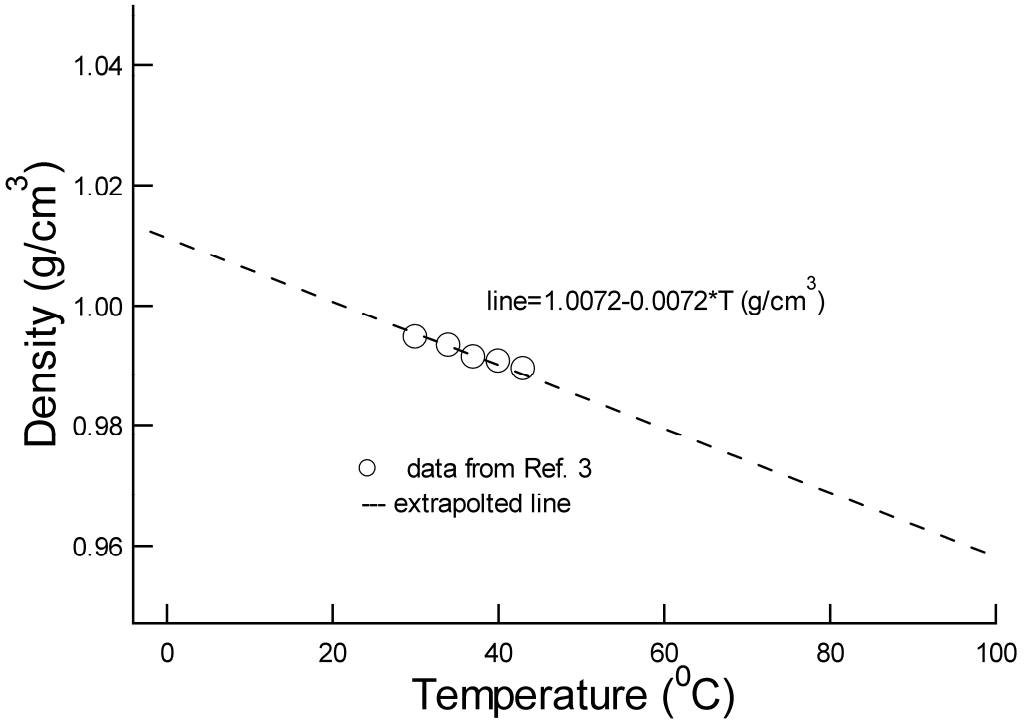

Figure 9. Showing the T-dependence of density at ambient pressure. The data (open circle) are from Ref. 12. The dashed line is the extrapolation from 0 to 100 °C.

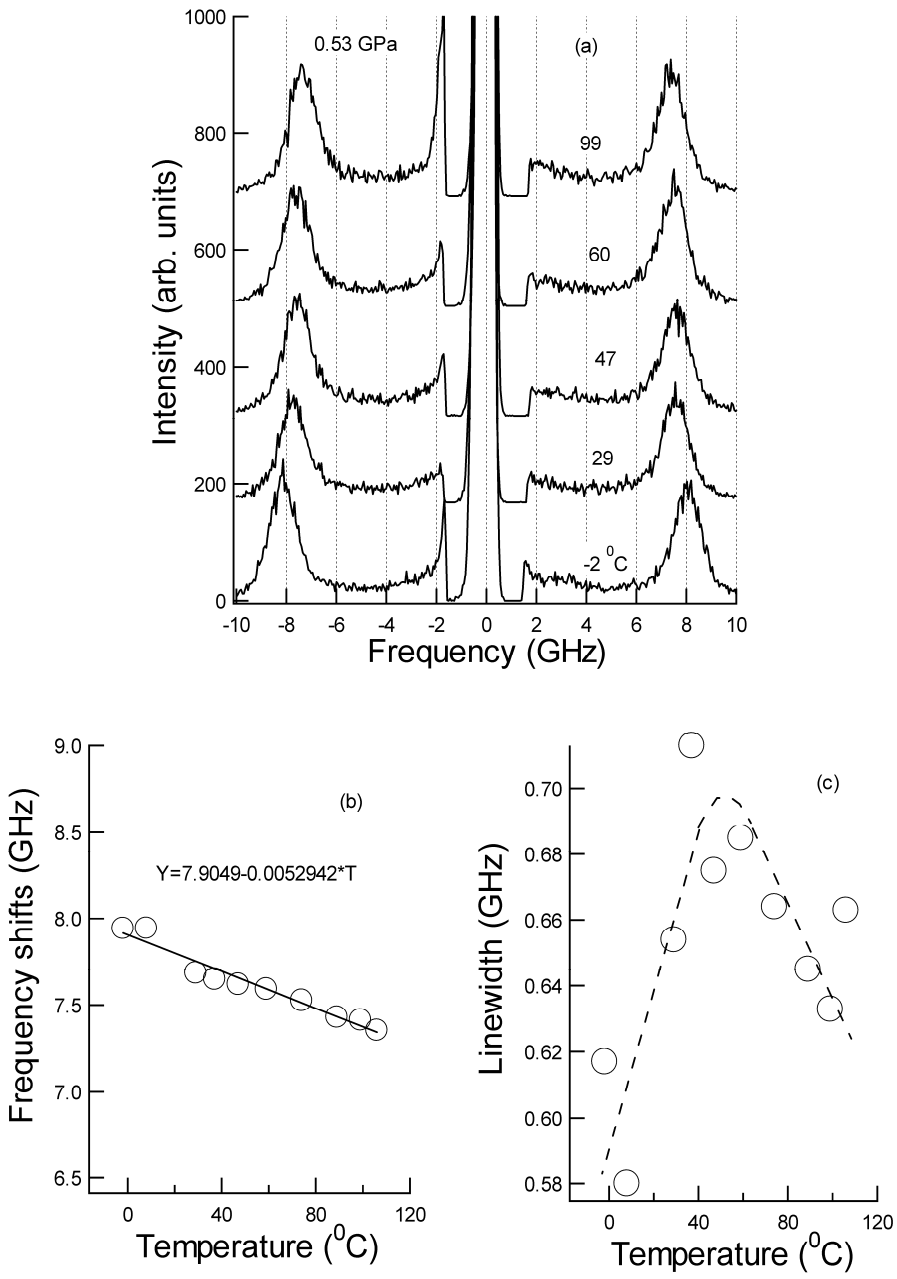

Figure 10. (a) The typical Brillouin spectra as the function of temperature at 0.53 GPa; (b) it shows the T-dependence of Brillouin frequency shifts. Symbols are data and solid line is the linear fit; (c) T-dependence of linewidth at 0.53 GPa. The behavior of linewidth relates to the relaxation process in the sample (Ref. 2). It is beyond the current study.

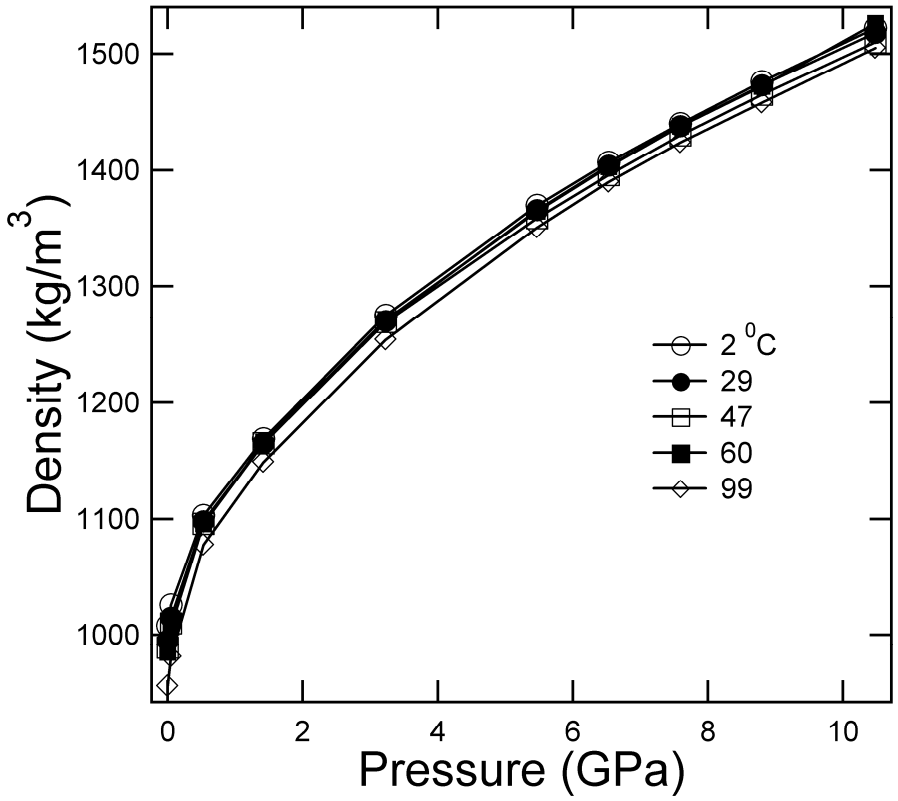

Figure 11. The calculated density via Eq. (3) at temperature -2, 29, 47, 60, and 100 °C between 0 and 12 GPa.

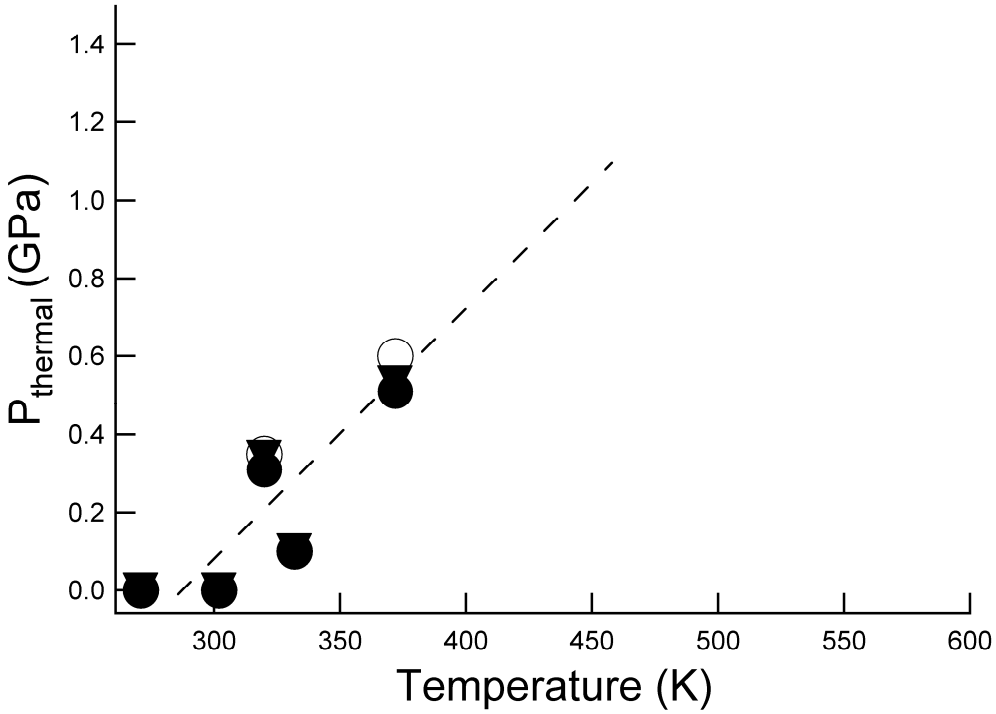

Figure 12. Thermal pressure as a function of temperature. Symbols are the data and dashed line is guide to eyes.

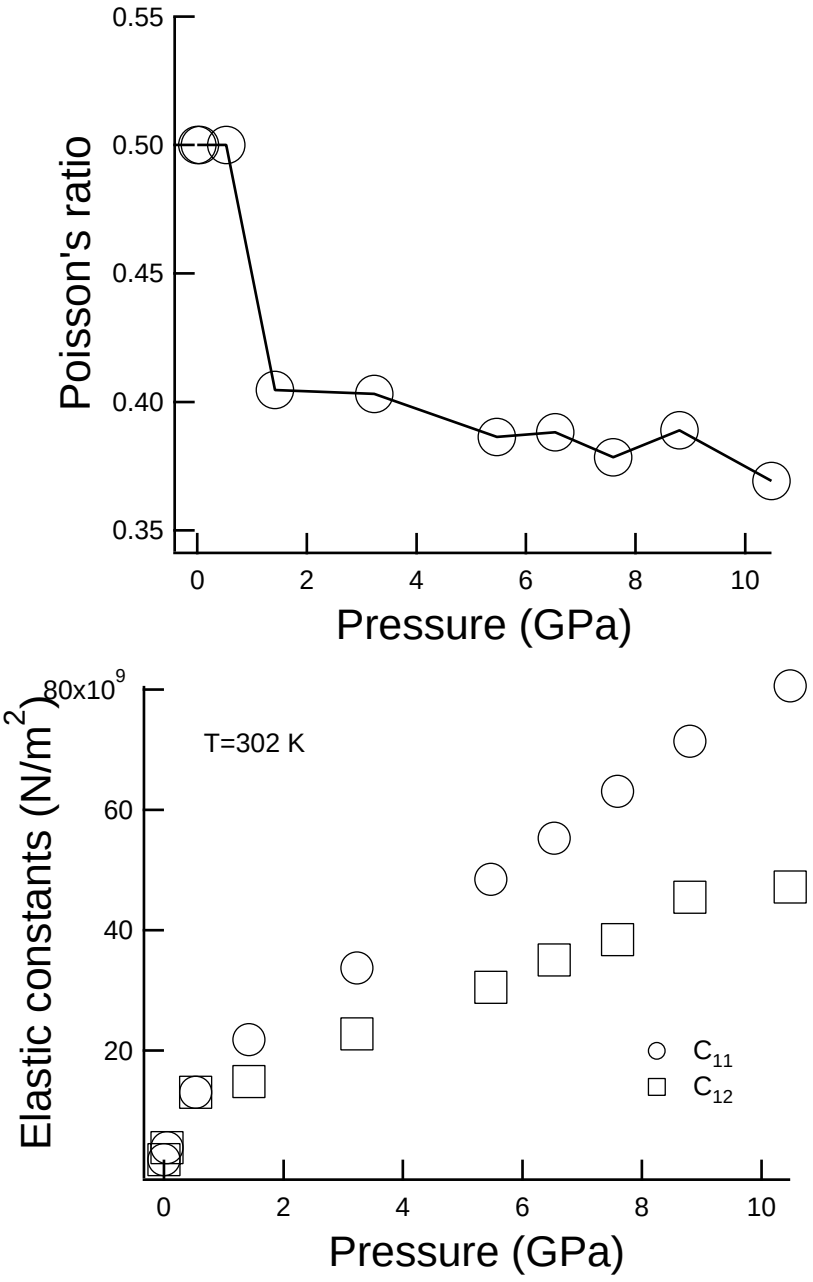

Figure 13. Pressure dependences of elastic constants and Poisson's ratio at room temperature.

Table I. Showing pressure, temperature, calculated density, volume, and bulk sound velocity, L-mode and T-mode velocities. The pressure has an averaged error of ± 0.2 GPa, the Brillouin has the error of 50 m/s in measurements.

Pressure (GPa)	Temperature (K)	Density (g/cm^3)	Volume (cm^3 /g)	Bulk velocity (m/s)	L-Mode (m/s)	T-Mode (m/s)
0	271	1.008	0.992	1434	1434	0
0.05	271	1.026	0.975	2029	2029	0
0.53	271	1.103	0.907	3562.45	3562.45	0
1.42	271	1.169	0.855	3818.84	4479.19	2027.23
3.23	271	1.275	0.784	4563.02	5314.3	2359.12
5.47	271	1.370	0.73	5214.68	6041.32	2641.68
6.53	271	1.407	0.711	5518.34	6387.11	2785.2
7.59	271	1.440	0.694	5758.35	6714.97	2991.51
8.8	271	1.476	0.678	5905.13	6872.84	3045.33
10.48	271	1.522	0.657	6128.82	7137.9	3168.66
0	302	0.995	1.005	1363	1363	0
0.05	302	1.015	0.985	1953	1953	0
0.53	302	1.098	0.911	3446.29	3446.29	0
1.42	302	1.165	0.858	3835.69	4325.35	1731.22
3.23	302	1.270	0.787	4561.45	5153.28	2076.56
5.47	302	1.366	0.732	5169.93	5957.45	2563.64
6.53	302	1.404	0.712	5456.99	6274.54	2682.04
7.59	302	1.438	0.695	5695.81	6624.54	2929.16
8.8	302	1.473	0.679	6062.53	6964.78	2969.08
10.48	302	1.518	0.659	6199.21	7288.15	3318.91
0	320	0.989	1.011	1322	1322	0

0.05	320	1.010	0.990	1912	1912	0
0.53	320	1.096	0.912	3417.13	3417.13	0
1.42	320	1.165	0.858	3788.61	4315.48	1789.52
3.23	320	1.269	0.788	4718.39	5248.23	1984.17
5.47	320	1.359	0.736	5288.03	6030.1	2509.82
6.53	320	1.396	0.716	5414.8	6268.71	2735.41
7.59	320	1.430	0.699	5732.36	6631.99	2888.35
8.8	320	1.465	0.683	6048.95	7002.01	3054.3
10.48	320	1.510	0.662	6174.05	7196.66	3202.3
0	333	0.985	1.015	1291	1291	0
0.05	333	1.007	0.993	1881	1881	0
0.53	333	1.096	0.912	3379.46	3379.46	0
1.42	333	1.166	0.858	3802.98	4270.63	1682.78
3.23	333	1.271	0.787	4608.61	5193.87	2074.32
5.47	333	1.365	0.733	5231.62	6014.63	2569.91
6.53	333	1.403	0.713	5357.81	6205.92	2712.09
7.59	333	1.438	0.695	5593.97	6530.18	2917.73
8.8	333	1.472	0.679	6120.7	7108.98	3131.44
10.48	333	1.526	0.655	6103.42	7126.24	3185.71
0	372	956	1.046	1199	1199	0
0.05	372	981	1.019	1789	1789	0
0.53	372	1078	0.928	3325.64	3325.64	0
1.42	372	1149	0.870	3835.69	4325.35	1731.22
3.23	372	1254	0. 797	4553.76	5196.79	2168.51
5.47	372	1351	0. 740	5125.56	5897.35	2525.96

6.53	372	1390	0.719	5369.97	6236.86	2747.07
7.59	372	1424	0. 702	5800.99	6778.21	3036.36
8.8	372	1458	0. 686	6193.81	7145.53	3085.69
10.48	372	1505	0. 664	6126.47	7127.14	3153.86

Table II: Bulk modulus, its derivative, initial volume, thermal expansion coefficient, and the temperature derivative of bulk modulus at ambient pressure are obtained via high-temperature Vinet EOS fit.

	271 K	302 K	320 K	333 K	372 K
K_{0T} (GPa)	5.42 ±0.4	5.2 (fix)	5.9 ±0.6	8.1 ±0.7	3.4 ±0.4
K_{0T}'	8.1 ±0.4	8.3 (fix)	7.8 ±0.4	6.8 ±0.4	9.3 ±0.6
V_{0T} (cm^3/g)	0.991 ±0.003	0.996(fix)	0.991 ±0.008	0.965 ±0.005	1.039 ±0.005
α_0 (10^{-5} K^{-1})		32.3 ± 4.6			
α_1		0			
$(\partial K_T / \partial T)_P$		-0.008±0.002			

Table III: The initial density is set to fixed number, the Vinet EOS fit yields the bulk modulus and its derivative.

	271 K	302 K	320 K	333 K	372 K
K_{0T} (GPa)	5.4 ±0.3	4.6 ±0.3	4.7 ±0.3	3.5 ±0.4	3.1 ±0.3
K_{0T}'	8.1 ±0.3	8.7 ±0.5	8.4 ±0.4	9.8 ±0.6	9.6 ±0.5
V_{0T} (cm^3/g)	0.992 (fix)	1.004 ±0.002	1.011 (fix)	1.015 (fix)	1.046 (fix)
α_0 (10^{-5} K^{-1})		40.4 ± 4.6			
α_1		0			
$(\partial K_T / \partial T)_P$		-0.009±0.002			

Table IV: High temperature Vinet EOS fitted to the P-V-T data. The recalculated pressures were shown in table. Fitting parameter: K_0=4.6 +/- 0.2 GPa, K_0'=8.7 +/- 0.2, V_0=1.004 +/- 0.002 cm^3/g, α_0=(40.4 +4.0) $\times 10^{-5}$ K^{-1}, and $(\frac{\partial K_T}{\partial T})_P$ = -0.009 +/- 0.002 $GPaK^{-1}$.

Reference temperature = 302.00 K, Pressure in GPa.

V (cm^3/g)	T (K)	P (obs)	P (calc)	ΔP
0.9920	271.0	0.0000	-0.0013	0.0013
0.9747	271.0	0.0500	0.0913	-0.0413
0.9066	271.0	0.5300	0.6429	-0.1129

0.8554	271.0	1.4200	1.3522	0.0678
0.7843	271.0	3.2300	3.0666	0.1634
0.7299	271.0	5.4700	5.3473	0.1227
0.7107	271.0	6.5300	6.4595	0.0705
0.6944	271.0	7.5900	7.5687	0.0213
0.6775	271.0	8.8000	8.9129	-0.1129
0.6570	271.0	10.4800	10.8473	-0.3673
1.0050	302.0	0.0000	-0.0036	0.0036
0.9852	302.0	0.0500	0.0952	-0.0452
0.9107	302.0	0.5300	0.6810	-0.1510
0.8584	302.0	1.4200	1.4021	0.0179
0.7874	302.0	3.2300	3.0961	0.1339
0.7321	302.0	5.4700	5.3889	0.0811
0.7123	302.0	6.5300	6.5271	0.0029
0.6954	302.0	7.5900	7.6686	-0.0786
0.6789	302.0	8.8000	8.9723	-0.1723
0.6588	302.0	10.4800	10.8541	-0.3741
1.0111	320.0	0.0000	0.0019	-0.0019
0.9901	320.0	0.0500	0.1040	-0.0540
0.9124	320.0	0.5300	0.7088	-0.1788
0.8584	320.0	1.4200	1.4565	-0.0365
0.7880	320.0	3.2300	3.1435	0.0865
0.7358	320.0	5.4700	5.2703	0.1997
0.7163	320.0	6.5300	6.3551	0.1749
0.6993	320.0	7.5900	7.4706	0.1194
0.6826	320.0	8.8000	8.7460	0.0540
0.6623	320.0	10.4800	10.5860	-0.1060
1.0152	332.0	0.0000	0.0053	-0.0053
0.9930	332.0	0.0500	0.1110	-0.0610
0.9124	332.0	0.5300	0.7382	-0.2082
0.8576	332.0	1.4200	1.5040	-0.0840
0.7868	332.0	3.2300	3.2251	0.0049
0.7326	332.0	5.4700	5.4834	-0.0134
0.7128	332.0	6.5300	6.6217	-0.0917
0.6954	332.0	7.5900	7.7974	-0.2074
0.6794	332.0	8.8000	9.0632	-0.2632
0.6553	332.0	10.4800	11.3422	-0.8622
1.0460	372.0	0.0000	-0.0466	0.0466
1.0194	372.0	0.0500	0.0554	-0.0054
0.9276	372.0	0.5300	0.6705	-0.1405
0.8703	372.0	1.4200	1.3938	0.0262
0.7974	372.0	3.2300	3.0086	0.2214
0.7402	372.0	5.4700	5.2162	0.2538
0.7194	372.0	6.5300	6.3315	0.1985
0.7022	372.0	7.5900	7.4222	0.1678
0.6859	372.0	8.8000	8.6300	0.1700
0.6644	372.0	10.4800	10.5047	-0.0247

FITTING STATISTICS FOR 5 PARAMETERS FITTED TO 55 DATA:

Ru= 2.8227% Rw= 4.5488%
CHI^2 (NON-WEIGHTED)= 0.0347 CHI^2 (WEIGHTED)= 121.9185
SUM(NON-W DIFFS^2)= 1.73353 SUM(W-DIFFS^2)= 6095.9230
MAXIMUM DELTA-PRESSURE=-0.862

Table V. The Mie-Gruneisen fitting results: K_0=4.9 GPa (room-T), K_0'=8.2 (room-T), V_0=1.005 (cm^3/g), Debye temperature θ_0 =150 K (fix), q=1 (fix), Gruneisen parameter γ=0.17 ± 0.10. In table: V is observed volume, P is observed pressure, Pcalc is calculated pressure, ΔP=P-Pcalc, and ΔPthermal=thermal pressure.

V(cm^3/g)	T(K)	P GPa	P(calc),	ΔP	$\Delta P_{Thermal}$(calc)
0.992	271.	0.00	-0.05	0.05	-0.07
0.975	271.	0.05	0.05	0.00	-0.12
0.907	271.	0.53	0.65	-0.12	-0.23
0.855	271.	1.42	1.38	0.04	-0.08
0.784	271.	3.23	3.11	0.12	0.00
0.730	271.	5.47	5.34	0.13	0.01
0.711	271.	6.53	6.41	0.12	0.00
0.694	271.	7.59	7.47	0.12	0.01
0.677	271.	8.80	8.73	0.07	-0.05
0.657	271.	10.48	10.55	-0.07	-0.19
1.005	302.	0.00	0.01	-0.01	0.00
0.985	302.	0.05	0.11	-0.06	-0.06
0.911	302.	0.53	0.73	-0.20	-0.19
0.858	302.	1.42	1.46	-0.04	-0.03
0.787	302.	3.23	3.14	0.09	0.10
0.732	302.	5.47	5.35	0.12	0.12
0.712	302.	6.53	6.44	0.09	0.10
0.695	302.	7.59	7.52	0.07	0.08
0.679	302.	8.80	8.75	0.05	0.06
0.659	302.	10.48	10.50	-0.02	-0.02
1.011	320.	0.00	0.05	-0.05	0.03
0.990	320.	0.05	0.16	-0.11	-0.03
0.912	320.	0.53	0.78	-0.25	-0.17
0.858	320.	1.42	1.53	-0.11	-0.03
0.788	320.	3.23	3.19	0.04	0.12
0.736	320.	5.47	5.24	0.23	0.31
0.716	320.	6.53	6.28	0.25	0.33
0.699	320.	7.59	7.33	0.26	0.34
0.683	320.	8.80	8.53	0.27	0.35
0.662	320.	10.48	10.25	0.23	0.31
1.015	332.	0.00	0.08	-0.08	0.05
0.993	332.	0.05	0.19	-0.14	-0.01
0.912	332.	0.53	0.83	-0.30	-0.17
0.858	332.	1.42	1.59	-0.17	-0.04
0.787	332.	3.23	3.28	-0.05	0.08
0.733	332.	5.47	5.45	0.02	0.15
0.713	332.	6.53	6.53	0.00	0.13
0.695	332.	7.59	7.64	-0.05	0.08
0.679	332.	8.80	8.83	-0.03	0.10
0.655	332.	10.48	10.96	-0.48	-0.35
1.046	372.	0.00	0.13	-0.13	0.17
1.019	372.	0.05	0.23	-0.18	0.12
0.928	372.	0.53	0.84	-0.31	-0.01

0.870	372.	1.42	1.55	-0.13	0.17
0.797	372.	3.23	3.12	0.11	0.40
0.740	372.	5.47	5.25	0.22	0.52
0.719	372.	6.53	6.31	0.22	0.51
0.702	372.	7.59	7.35	0.24	0.53
0.686	372.	8.80	8.49	0.31	0.60
0.664	372.	10.48	10.27	0.21	0.51

STANDARD DEVIATION: 0.162514